Iraqi Journal of Science, 2022, Vol. 63, No. 8, pp: 3402-3411
DOI: 10.24996/ijs.2022.63.8.16

ISSN: 0067-2904

Surface Plasmon Resonance (SPR) Simulation of a Gold-Bismuth Bi-layer Gas Sensor

Ruqayah A. Ulwali[1]* , Heba Kh. Abbas[1] , Ali J Karam [2], Ali A. Al-Zuky[3] , Mahasin F. Hadi Al-Kadhemy[3] , Anwar H. Al-Saleh[4]

[1]*Department of Physics, College of Science for Women, University of Baghdad, Baghdad, Iraq*
[2] *Department of Information Technology ,College of Computer and Information Technology, University of Garmian ,Kurdistan Region, Iraq.*
[3]*Department of Physics , Collage of Science, Mustansiriya University, Baghdad, Iraq.*
[4]*Department of Computer Science , Collage of Science, Mustansiriya University, Baghdad ,Iraq.*

Received: 29/3/2021 Accepted: 19/3/2022 Published: 30/8/2022

Abstract

The features of plasmonic surface frequency sensor technology, such as the small number of sensor samples required, electromagnetic interference, and high sensitivity, have been found to be highly important.. In this paper, a simulation program was created in Matlab_b2018 by adopting Fresnel equations for calculating the reflectivity of the electromagnetic wave between different media. A surface plasmon resonance sensor based on electromagnetic wavelengths within the range (100 nm to 1000 nm) has been proposed. The transfer matrix was used for a system consisting of four different media. The first medium is a semicircular BK7 glass prism, the second medium is a gold layer (40 nm thick), then a bismuth layer of variable thicknes(10–80) nm, and the last medium is air as the sensing medium. The surface plasmon resonance (SPR) technique was adopted based on the Kretschmann configuration in the simulation of the proposed system. The simulation results showed that there is no SPR within the range of wavelengths (100-500nm), while SPR appears in the visible region and in the IR region at wavelengths (900 and 1000nm). The SPR phenomenon starts to weaken gradually with an increase in the thickness of the bismuth layer. The full width at half maximum (FWHM) decreases with the decrease of thickness of bismuth layer. The best value for it is (10) at thickness (d=10 nm) and wavelength (900 nm). While the height (H) of the SPR dip increased, with the best value of (0.95) at thickness (d=10 nm) and wavelength (700 nm). Also, the sensitivity increased with increasing the bismuth layer thickness at wavelengths (700 , 800,
and 1000) nm. The highest obtained sensitivity(S) was (112.5 deg/RIU).

Keywords: Surface plasmon resonance sensor, Au layer, bismuth layer, Kretschmann's configuration.

محاكاة رنين البلازمون السطحي (SPR) للذهب – البزموت كمستشعر للغاز

رقية عبد الولي[1*] , هبة خضير عباس [1] , علي جبار كرم[2] , علي عبد داوود الزكي[3] , محاسن فاضل هادي الكاظمي[3] ، انوار حسن مهدي الصالح[4]

[1] قسم الفيزياء , كلية العلوم للبنات , جامعة بغداد , بغداد , العراق .

*Email: ruqayah.a@csw.uobaghdad.edu.iq

[2] قسم تكنلوجيا المعلومات ,كلية الحاسوب وتكنلوجيا المعلومات ،جامعة كرميان ،أقليم كردستان ، العراق .

[3] قسم الفيزياء , كلية العلوم , الجامعة المستنصرية , بغداد , العراق .

[4] قسم علوم الحاسوب , كلية العلوم , الجامعة المستنصرية , بغداد , العراق .

الخلاصه

لقد وجدت ميزات تقنية مستشعر تردد السطح البلازموني ، مثل العددالقليل لعينات المستشعر المطلوبة ، التداخل الكهرومغناطيسي والحساسية العالية ، أنها مهمة للغاية في هذا الوقت . في هذا البحث ، تم إنشاء محاكاة باستخدام برنامج Matlab_b2018 باعتماد معادلات فرينل لحساب انعكاسية الموجة الكهرومغناطيسية بين الاوساط المختلفة. تم اقتراح مستشعر تردد الرنين البلازموني يعتمد على أطوال موجات كهرومغناطيسية ضمن النطاق (100 نانومتر إلى 1000 نانومتر) . تم استخدام مصفوفة النقل لنظام يتكون من أربع اوساط مختلفة، الوسط الأول عبارة عن موشور زجاجي نصف دائري BK7 ، الوسط الثاني طبقة من الذهب ذات السمك 40 نانومتر ، ثم طبقة بسمك متغير من البزموت (10–80) نانومتر ، والوسط الأخيرهو الهواء (وسط الاستشعار). تم اعتماد تقنية الرنين السطحي البلازموني (SPR) بناءً على تكوين Kretschmann في محاكاة النظام المقترح. أظهرت نتائج المحاكاة عدم وجود SPR ضمن الأطوال الموجية (100–500) نانومتر ، بينما يظهر SPR في المنطقة المرئية وفي منطقة الأشعة تحت الحمراء عند الاطوال الموجية (900 و 1000) نانومتر. بينما بدأت ظاهرة SPR في الضعف تدريجياً مع زيادة سمك طبقة البزموت. أضهر عرض القمة عند منتصف الارتفاع (FWHM) تناقص مع انخفاض سمك طبقة البزموت ، لذلك وجدت أفضل قيمة له (10) عند السمك (d = 10 نانومتر) والطول الموجي (900 نانومتر)، بينما أضهرت زيادة في ارتفاع القمة (H) لمنحني الـ SPR ، وكانت أفضل قيمة له (0,95) عند السُمك (d = 10 نانومتر) والطول الموجي (700 نانومتر). كما أبدت الحساسية للمستشعرزيادة مع زيادة السمك عند الاطوال الموجية (700 ، 800 ، 1000) نانومتر ، وكانت أعلى حساسية تم الحصول عليها (S = 112.5 deg/RIU).

1. Introduction

Recently, optical sensors have played an important role in many applications, for instance, in detecting chemical and biological pollutants in fluids, due to the high development in optical sensing technology [1]. Different optical sensors have been designed to reduce time and cost and enhance daily processes [2]. Building applied process systems are often costly and require much effort and time. Therefore, many scientists in many fields have resorted to the use of simulation techniques for different practical systems. Simulation is the study and construction of models or programs that adopt methods to approximate and imitate a physical or real life system to study the expected results of the system and its potential use in practical applications. The simulation system simulates a reality that is sometimes difficult to provide due to costs and human capabilities [3-5]. Therefore, the principle of plasmonic surface (SPR) frequency of the plasmonic surface (SPR) is used for this purpose, which occurs when the frequency of the incident ray equals the frequency of the wave of the plasmonic surface (SPW). The plasmonic behavior of various surface shapes, such as circles, squares, and flat surfaces, can be studied and tested using simulation software [6-9]. SPR principle was used in different areas, such as optics technology, non-linear optics, and microscopy, in a circuit that combines two different signals and spectroscopy [10-12].

Researchers are intensifying their efforts to design and develop new sensors that meet current and future demands and applications to improve the sensitivity of (SPR) sensors. Many studies have worked by adding layers of semiconductor and insulating materials as well as metamaterials.

Vahed and Nadri [13] designed Air/MoS2/ Nanocomposite/ MoS2/ graphene which acts as an optical biosensor using Otto-configuration. A high sensitivity value was obtained (200 deg /RIU) and evaluated with six layers of MoS2 and a nano-composite layer containing (Au NPs)

and TiO2, which acted as the host electrical insulator. Lin et al. [14] proposed an (SPR) sensor depending on two-dimensional materials (graphene, MoS2, WS2 and WSe2) with various metal films (Au, Ag or Cu) to enhance the sensitivity. The results showed high sensitivity values of 159, 194 or 155°/RIU for Au, Ag or Cu, respectively.

In this study, Kretschmann configuration was used to simulate plasmonic surface resonance (SPR) of a system consisting of gold and bismuth layers placed on a semicircular glass prism for a wide range of the electromagnetic spectrum ranging from the ultraviolet to the infrared region (the electromagnetic wavelengths used were in range (100-1000) nm). Also, the spectrum regions of SPR were determined. In addition, the full width at half maximum (FWHM) of the SPR dip and the sensitivity (S) of the proposed system were calculated by changing the refractive index (Δn) of the sensing medium (i.e. the air), where (Δn=0, 0.04 0.08, and 0.12).

2. Surface Plasmon Resonance Sensor Theory Concepts

Using multilayer structures arranged on a prism, planar, grating, or cylindrical waveguides topped with a thin metallic layer, (SPR) can happen[15]. The Otto[16] and Kretschmann arrangements [17] are metal-dielectric arrangements to prism coupling for (SPR) excitation . In the two configurations, the polarized light ray is reflected from the separating surface between the prism and the thin metal layer to be received by a sensitive detector. After that, the optical wave passes through the thin layer and generates a surface optical wave at the metal boundary[18].

The Kretschmann's arrangement was employed using metal film on a glass surface, and the surface plasmon wave spread constant (SPW) is show by equation [18] :

$$k_x = n_p k_0 \sin(\theta_{SPR}) = k_0 \sqrt{\frac{\epsilon_m n_a^2}{\epsilon_m + n_a^2}} \quad \ldots\ldots (1)$$

Where: kx is the wave vector, np is the prism refractive index, na is the sample refractive index and θSPR is the resonant angle that excites the surface plasmon , k0 = 2π/λ is the wave vector of incident light , λ is the free area wavelength, and ϵm= (ϵmr +j ϵmi) is the electrical insulator constant of a complex metal which is based on the wavelength . According to Equation (1), the conjugation condition (between k0 and SPW) is only fulfilled if |ϵ_mr| is more than (n_p^2 n_a^2)/(n_p^2-n_a^2). It happens when wavelength has been decreased, |ϵ_mr | represented approaches of critical value with SPW that cannot be excited [18]. The intensity's beam of polarized light can be accessed via matrix method utilizing Maxwell's and Fresnels equations [19]:

$$M_k = \begin{bmatrix} \cos(\beta_k) & -\frac{i}{q_k}\sin(\beta_k \\ -iq_k\sin(\beta_k) & \cos(\beta_k) \end{bmatrix} \quad \ldots\ldots (2)$$

Where M_k represents characteristic transfer matrix and as the same as the luminous spread through a layers , β_k is a phase agent , and q_k the cross magnetic incident ray , as shown by the following equations[19] :

$$\beta_k = k_0 d_k \sqrt{n_k^2 - n_p^2 \sin(\theta_i)^2} \quad \ldots\ldots (3)$$

$$q_k = \frac{\sqrt{n_k^2 - n_p^2 \sin(\theta_i)^2}}{n_k^2} \quad \ldots\ldots (4)$$

Where: dk represents the thickness of the kth layer, θi is the angle of incidence, nk is the kth layer refractive index which depends on wavelength. The total characteristic transfer matrix has been estimated via multiplication for each Mk matrix of kth layer index as shown[19] :

$$M_{total} = \prod_{k=1}^{N-1} M_k \quad \ldots\ldots (5)$$

The Fresnel reflection coefficient (r) for multilayers by M total matrix terms is estimated via [19] :

$$\boldsymbol{r(\theta_i, \lambda) = \frac{(M_{11}+M_{12}q_N)q_1-(M_{21}+M_{22}q_N)}{(M_{11}+M_{12}q_N)q_1+(M_{21}+M_{22}q_N)}} \quad \textbf{..... (6)}$$

Where M11, M12, M21 and M22 represent the components of M_total , q1 as well as qN are the cross magnetic incidence ray for the initial and the final layers, respectively. So, the reflectance (R) of a multilayer structure is given as [19] :

$$\boldsymbol{R = |r(\theta_i, \lambda)|^2} \quad \textbf{..... (7)}$$

The reflectance can be estimated depending on two principles:

The angular interrogation mode (AIM), when the angle of incidence changes but the wavelength remains constant.

The wavelength interrogation mode (WIM), where the incidence angle appears stable while the wavelength is different.

The suitable resonant angle of exciting SPR effect appears as in the following equation [20]:

θ_SPR= ⟦sin⟧ ^(-1)⟦(1/n_p √((ϵ_m n_a^2)/(ϵ_m+n_a^2)))⟧ ..... (8)

3. Methodology: Surface plasmon resonance sensor simulations

In this study, a simulation program was constructed in Matlab_b2018 by adopting the Fresnel equations of reflectivity of electromagnetic wavelengths. To the resonance conditions, p-polarized (TM) light must be used any change in the dielectric constant of the sensor medium (i.e. the change in the refractive index of the sensor medium) causes SPR bottom curve shift (when the reflectivity of the light is a function of the angle of incidence). As a result, the greater the change in the resonance angle, the greater the sensor's sensitivity (S), which is given by the following equation [21]:

$$\boldsymbol{S = \frac{\Delta\theta_{SPR}}{\Delta n} = \frac{\theta_{SPR1}-\theta_{SPR2}}{n_1-n_2}} \quad \textbf{..... (9)}$$

Where: $\Delta\theta_{SPR}$ represents the difference in resonance angle, and Δn is the difference in the refractive index of the sensor medium (form n_1 to n_2), causing a change in resonance angle from θ_{SPR1}, and θ_{SPR2}, respectively.

The suggested sensor of this study that adopts the resonance surface plasmon phenomenon is designed as shown in Figure 1.

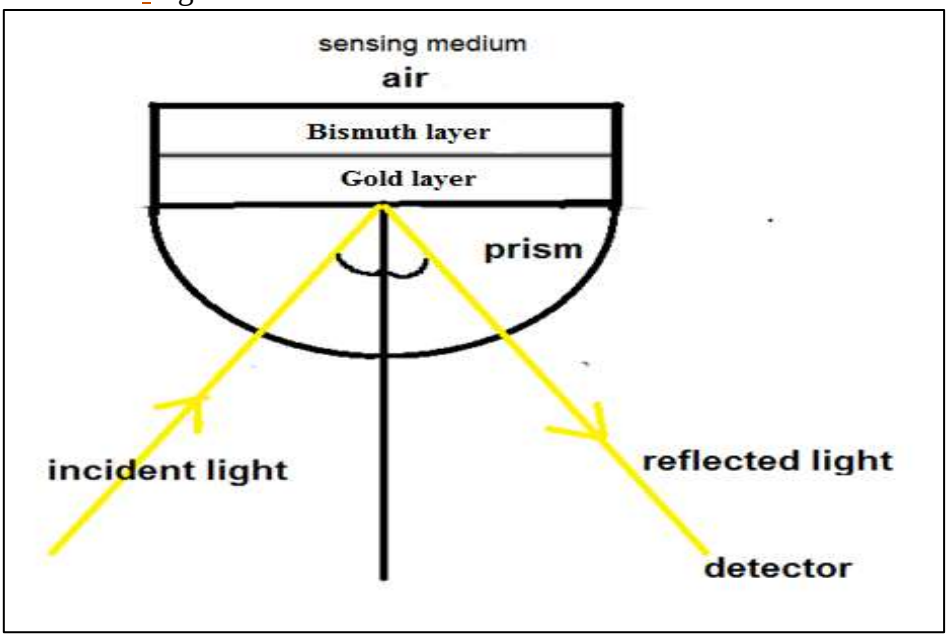

Figure 1- The proposed SPR sensor configuration.

The proposed sensor consists of a semi-circular (BK7) glass prism on which a 40nm thickness gold layer was deposited, a layer of bismuth, of variable thickness(10-80nm) was deposited on the gold layer and adopting the air as the sensation medium. The angle of incidence of light on the semicircular prism can be changed from (0 to 90) degrees. The refractive indices as a function of wavelength(100 to 1000)nm for the BK7 glass, gold, and bismuth were obtained (the refractive indexes tables were approved on the website https://refractiveindex.info) . To measure the reflectivity and how a slight change in the refractive index of the sensing medium affects to the resonance angle ,so, the refractive index (Δn) has been used (0, 0.04, 0.08, 0.12).

4. Results and Discussions

The proposed sensor system simulation of reflectivity is shown in Figure 2. It shows the change of reflectivity (R) as a function of the angle of the incident light on the prism for different values of wavelength (100-1000nm) and different values of the bismuth layer thickness(d)(10-80nm). These curves were obtained by implementing the Matlab simulation algorithm. The most important curves that show a significant change in the calculated reflectivity state were presented. For wavelengths from 100nm to 500nm, it was noted from the curves that the reflectivity was very low in the ultraviolet region and the initial part of the visible region; also there was no distinctive appearance of surface plasmon resonance (SPR). In the remaining part of the visible spectrum, the surface plasmon resonance was obtained strongly at 700 nm. While in the infrared region, the surface plasmon resonance was strong and very distinctive for wavelengths from 800nm to 1000nm. However, strong SPR dips at bismuth layer thicknesses from 10nm to 50nm were observed. While for bismuth thicknesses d=70 and 80 nm, the SPR dips were small.

For each wavelength and bismuth thickness, the reflectivity curves were analyzed to determine the sensor parameters (FWHM and the height (H) of the SPR dip). For the SPR dips, Figures 3 and 4 show the relationship between height H and FWHM as a function of bismuth layer thickness and electromagnetic wavelengths from 100nm to 1000nm. The sensitivity (S) of the proposed sensing device is shown in Figure 5 as a function of the bismuth layer thickness.

The results showed that the FWHM values of the SPR dips decreased and the height (H) values of the SPR dips increased as the bismuth layer thickness increased in the visible and infrared regions. The best value of FWHM was (10) at d=10 nm thickness and 900 nm wavelength. While the best value of the height (H) of the SPR dip was (0.95) at thickness d=10 nm and 700 nm wavelength. This information helped to determine the best bismuth thickness to be used in the sensor. Although the sensitivity (S) of the proposed device increased at wavelengths (700, 800, and 1000 nm) with increasing thickness, the highest sensitivity of 112.5 deg/RIU was obtained.

5. Conclusions

The results showed that there was no SPR within the wavelength range (100-500) nm, it was weak in the visible region but well in the (IR) region at wavelengths (900 and 1000) nm, and that the phenomenon of SPR weakens with the increase of the bismuth layer thickness. . FWHM also decreased as the thickness of the bismuth layer decreased and the height increased. With increasing the thickness at wavelengths (700, 800, and 1000 nm), the sensitivity improved. At 700nm and 800nm wavelengths and 10-60nm bismuth layer thickness, the highest sensitivity (S) of 112.5 deg/RIU was obtained

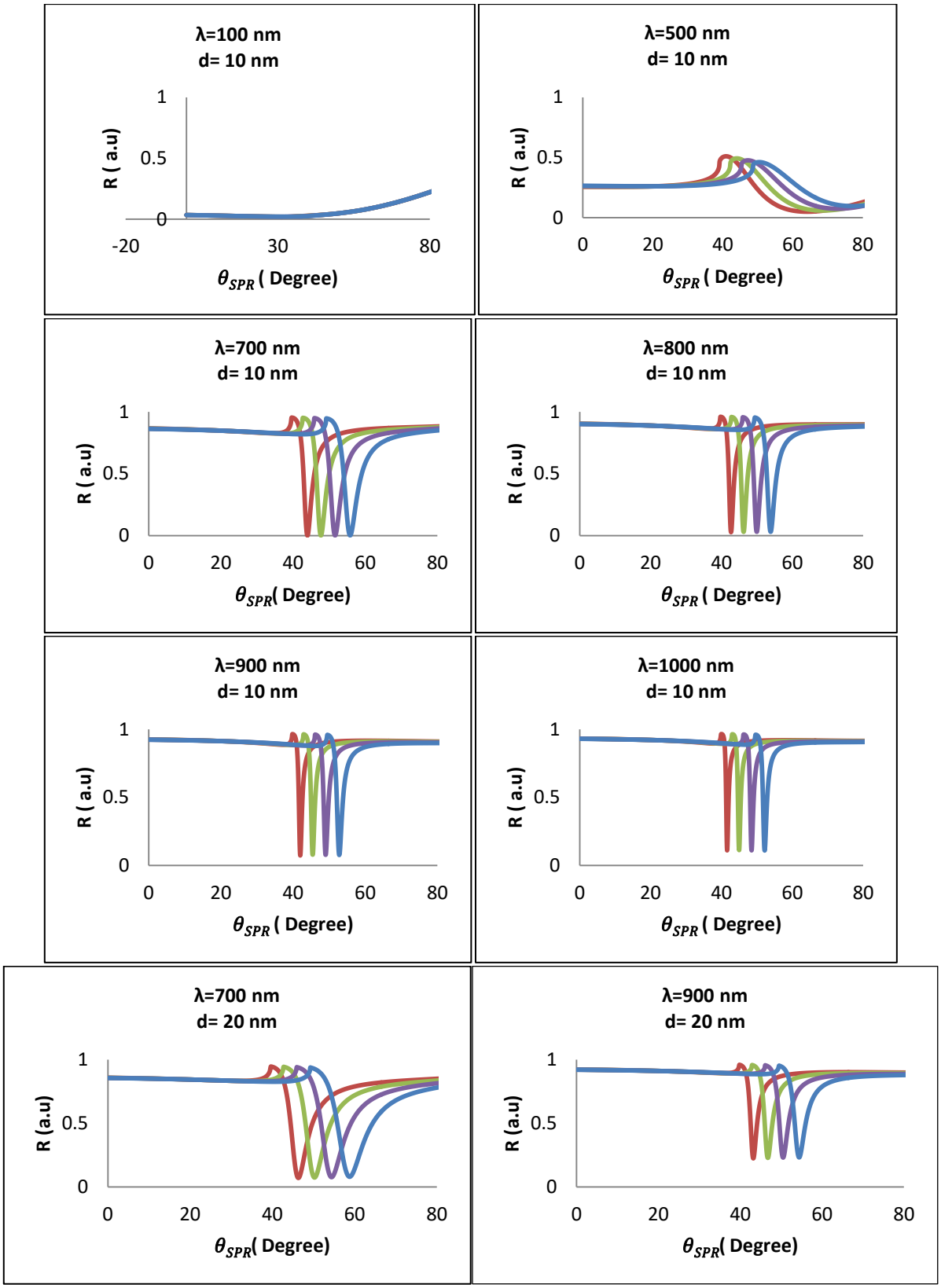
λ=100 nm
d= 10 nm
R (a.u)
1
0.5
0
-20
30
80
θ_{SPR} (Degree)
λ=500 nm
d= 10 nm
R (a.u)
1
0.5
0
0
20
40
60
80
θ_{SPR} (Degree)
λ=700 nm
d= 10 nm
R (a.u)
1
0.5
0
0
20
40
60
80
θ_{SPR}(Degree)
λ=800 nm
d= 10 nm
R (a.u)
1
0.5
0
0
20
40
60
80
θ_{SPR} (Degree)
λ=900 nm
d= 10 nm
R (a.u)
1
0.5
0
0
20
40
60
80
θ_{SPR} (Degree)
λ=1000 nm
d= 10 nm
R (a.u)
1
0.5
0
0
20
40
60
80
θ_{SPR} (Degree)
λ=700 nm
d= 20 nm
R (a.u)
1
0.5
0
0
20
40
60
80
θ_{SPR}(Degree)
λ=900 nm
d= 20 nm
R (a.u)
1
0.5
0
0
20
40
60
80
θ_{SPR}(Degree)

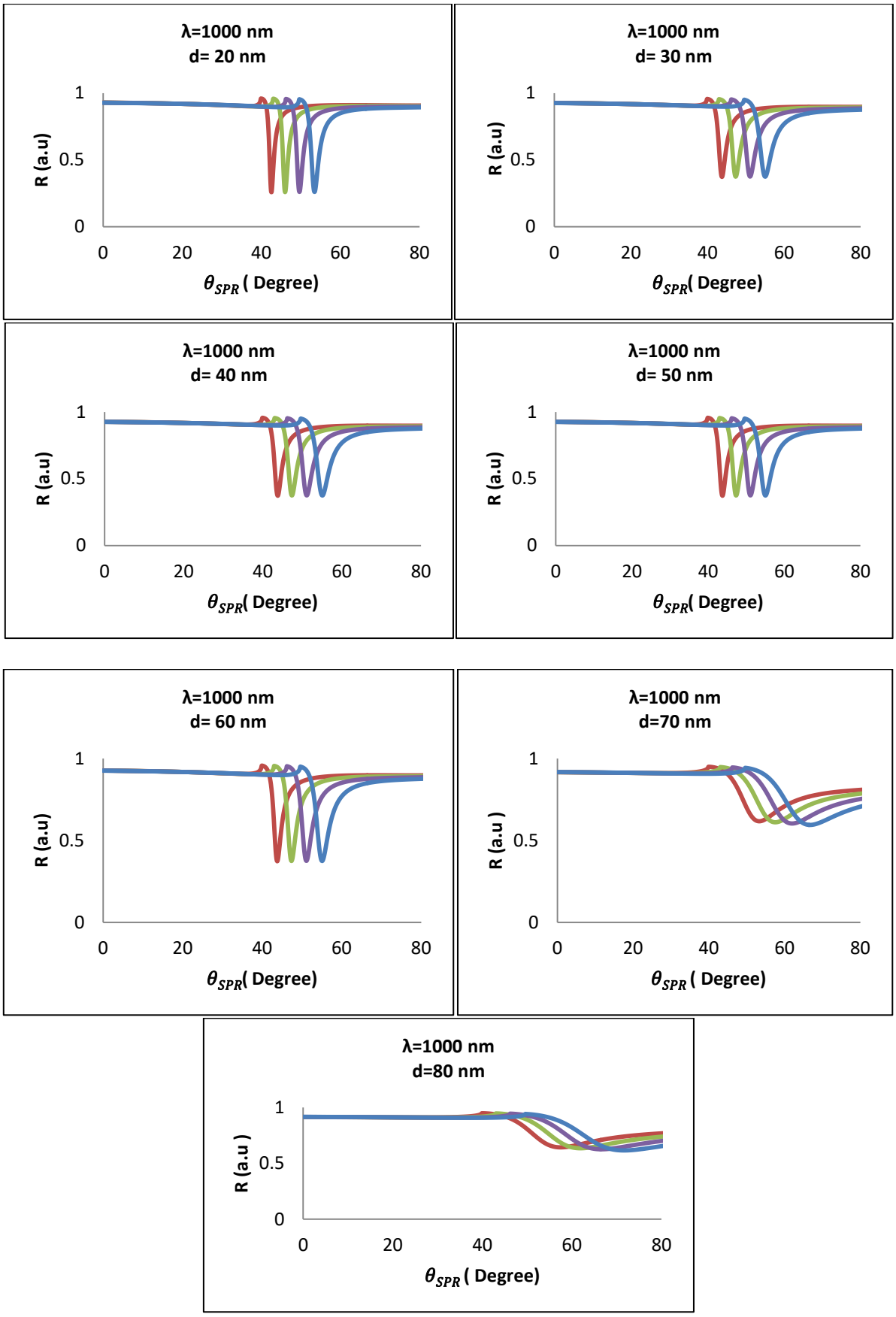

Figure 2-Surface Plasmon resonance sensor curves for different thicknesses of bismuth layers (10 -80 nm) at different incident wavelengths (100 -1000 nm) .

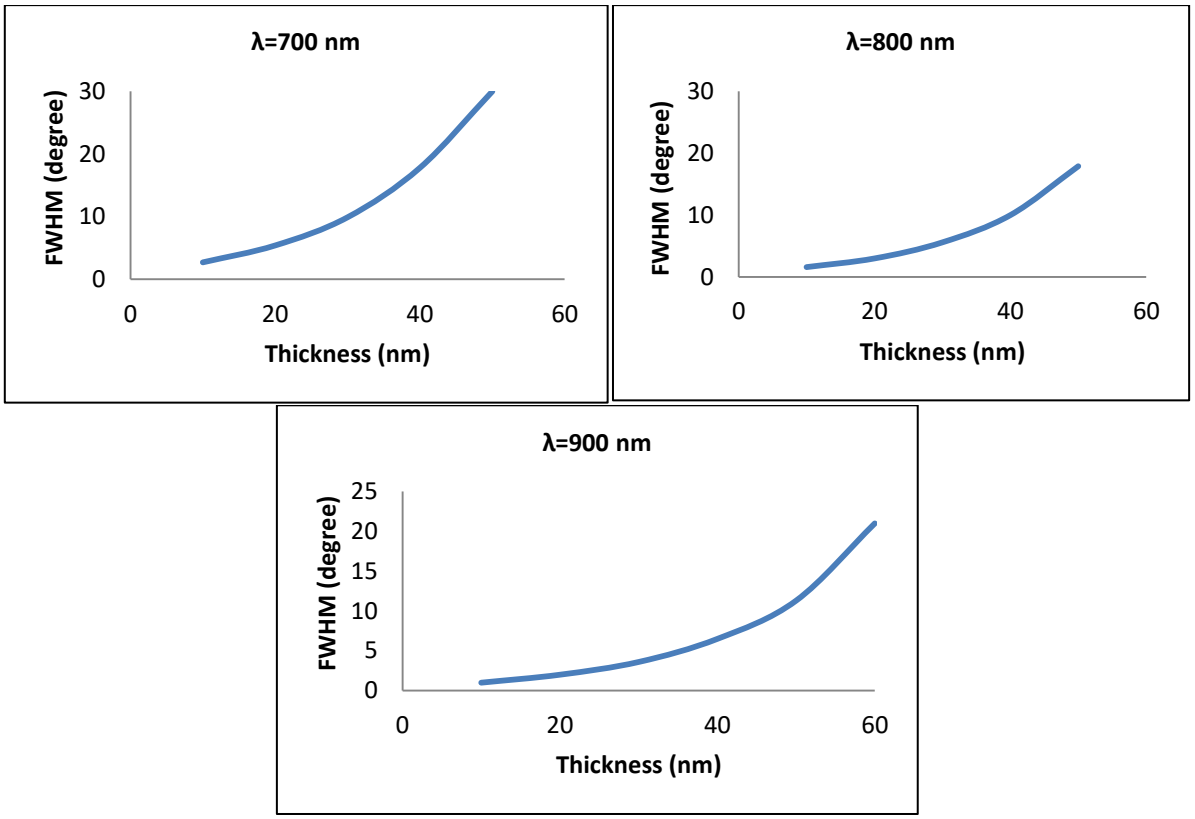

Figure 3-FWHM as a function of bismuth layer thickness for different wavelengths (100 - 1000 nm) .

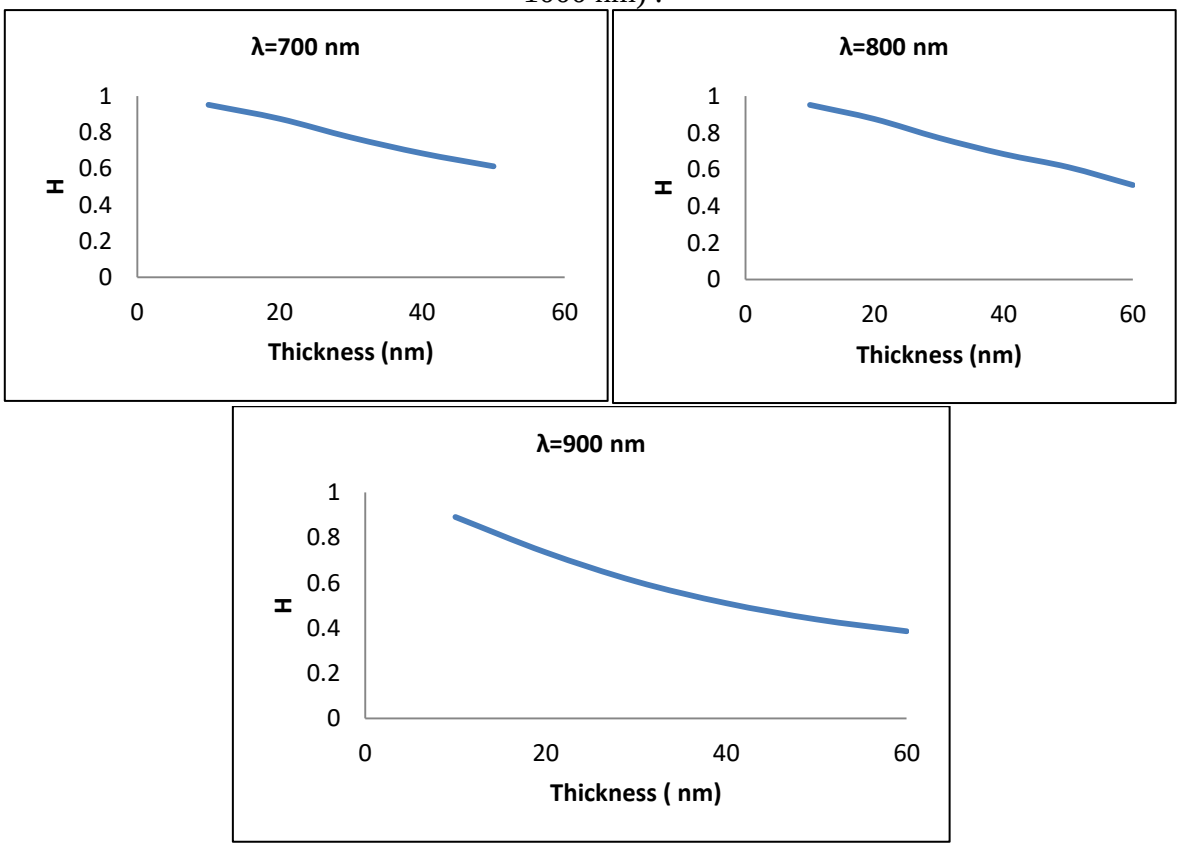

Figure 4-Height (H) of the SPR dip as a function of bismuth layer thickness at different wavelengths (100 -1000 nm) .

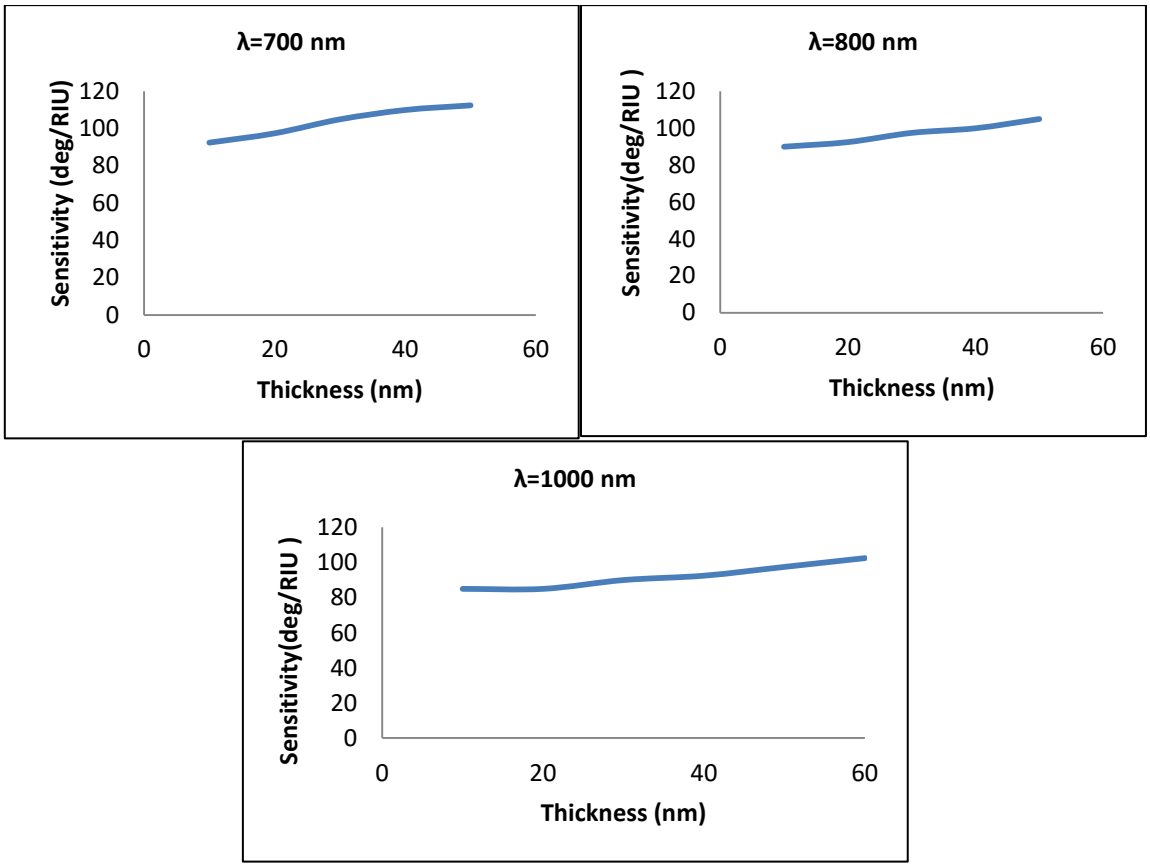

Figure 5- The sensitivity of sensor as a function of bismuth layer thickness at different wavelengths (100 -1000 nm) .

References

[1] Y. W. Fen, W. M. M. Yunus, Z. A. Talib, and N. A. Yusof, "Development of surface plasmon resonance sensor for determining zinc ion using novel active nanolayers as probe," *Spectrochimica Acta Part A: Molecular and Biomolecular Spectroscopy*, vol. 134, pp. 48-52, 2015.

[2] G. Jimenez-Cadena, J. Riu, and F. X. Rius, "Gas sensors based on nanostructured materials," *Analyst*, vol. 132, pp. 1083-1099, 2007.

[3] D. Van Der Leer, N. Weatherill, R. Sharp, and C. Hayes, "Modelling the diffusion of lead into drinking water," *Applied Mathematical Modelling*, vol. 26, pp. 681-699, 2002.

[4] N. H. Resham, H. K. Abbas, H. J. Mohamad, and A. H. Al-Saleh, "Noise Reduction, Enhancement and Classification for Sonar Images," *Iraqi Journal of Science*, pp. 4439-4452, 2021.

[5] H. K. Abbas, F. Faris, S. Sami, and A. Z. Fadel, "Adopting Image Integration Techniques to Simulate Satellite Images," *Iraqi Journal of Science*, pp. 3445-3455, 2020.

[6] S. Ghosh and M. Ray, "Analysis of silicon based surface Plasmon Resonance Sensors with different amino acids," *Silicon*, vol. 7, pp. 313-322, 2015.

[7] S. Pal, Y. Prajapati, J. Saini, and V. Singh, "Resolution enhancement of optical surface plasmon resonance sensor using metamaterial," *photonic sensors*, vol. 5, pp. 330-338, 2015.

[8] S. Singh, S. K. Mishra, and B. D. Gupta, "Sensitivity enhancement of a surface plasmon resonance based fibre optic refractive index sensor utilizing an additional layer of oxides," *Sensors and Actuators A: Physical*, vol. 193, pp. 136-140, 2013.

[9] S. Shukla, N. K. Sharma, and V. Sajal, "Sensitivity enhancement of a surface plasmon resonance based fiber optic sensor using ZnO thin film: a theoretical study," *Sensors and Actuators B: Chemical*, vol. 206, pp. 463-470, 2015.

[10] T. Srivastava, R. Das, and R. Jha, "Highly accurate and sensitive surface plasmon resonance sensor based on channel photonic crystal waveguides," *Sensors and Actuators B: Chemical,* vol. 157, pp. 246-252, 2011.

[11] W. Robertson and M. May, "Surface electromagnetic wave excitation on one-dimensional photonic band-gap arrays," *Applied physics letters,* vol. 74, pp. 1800-1802, 1999.

[12] W. Su, G. Zheng, and X. Li, "A resonance wavelength easy tunable photonic crystal biosensor using surface plasmon resonance effect," *Optik,* vol. 124, pp. 5161-5163, 2013.

[13] H. Vahed and C. Nadri, "Sensitivity enhancement of SPR optical biosensor based on Graphene–MoS2 structure with nanocomposite layer," *Optical Materials,* vol. 88, pp. 161-166, 2019.

[14] Z. Lin, S. Chen, and C. Lin, "Sensitivity Improvement of a Surface Plasmon Resonance Sensor Based on Two-Dimensional Materials Hybrid Structure in Visible Region: A Theoretical Study," *Sensors,* vol. 20, p. 2445, 2020.

[15] D. M. Hernández, J. Velázquez-González, D. Luna-Moreno, M. Torres-Cisneros, and I. Hernández-Romano, "Prism-based surface plasmon resonance for dual-parameter sensing," *IEEE Sensors Journal,* vol. 18, pp. 4030-4037, 2018.

[16] E. B. Costa, E. P. Rodrigues, and H. A. Pereira, "Sim-SPR: An open-source surface plasmon resonance simulator for academic and industrial purposes," *Plasmonics,* vol. 14, pp. 1699-1709, 2019.

[17] E. Kretschmann and H. Raether, "Radiative decay of non-radiative surface plasmons excited by light," *Z. Naturforsch. a,* vol. 23, pp. 2135-2136, 1968.

[18] J. Homola, I. Koudela, and S. S. Yee, "Surface plasmon resonance sensors based on diffraction gratings and prism couplers: sensitivity comparison," *Sensors and Actuators B: Chemical,* vol. 54, pp. 16-24, 1999.

[19] J. Banerjee, M. Bera, and M. Ray, "Theoretical differential phase analysis for characterization of aqueous solution using surface plasmon resonance," *Plasmonics,* vol. 12, pp. 1787-1796, 2017.

[20] M. Cook, *Commanding right and forbidding wrong in Islamic thought*: Cambridge University Press, 2001.

[21] S. Fouad, S. Naseer, Z. Jamal, and P. Poopalan, "Enhanced sensitivity of surface plasmon resonance sensor based on bilayers of silver-barium titanate," *Журнал нано-та електронної фізики,* pp. 04085-1-04085-5, 2016.